Int. J. Electrochem. Sci., 10 **(2015)** 4241 - 4251

International Journal of
ELECTROCHEMICAL
SCIENCE
www.electrochemsci.org

Effect of Tartaric Acid Concentration on the Anodic Behaviour of Titanium Alloy

Chunjuan Fu, Hongxing Liang[*], *Mei Yu, Jianhua Liu, Songmei Li*

School of Materials Science and Engineering, Beihang University, Beijing 100191, China
[*]E-mail: hongxingliang@buaa.edu.cn

Received: 22 December 2014 / *Accepted:* 31 March 2015 / *Published:* 23 March 2015

Ti-6.5Al-1Mo-1V-2Zr titanium alloy specimens have been anodized in sulfuric acid and tartaric acid/sulfuric acid. The effect of tartaric acid concentration on anodic behavior of sulfuric acid anodic film was investigated by Scanning electron microscopy (SEM), Raman spectra and electrochemical technique. It was found that 30g/L tartaric acid addition increased the thickness of anodic film, decreased the crystallinity and weakened the dissolution rate of anodic film. However, 90g/L tartaric acid addition caused the opposite trends to emerge: thickness of anodic film was reduced. The anodic film dissolution rate in sulfuric acid with 90g/L tartaric acid is faster than that in sulfuric acid with 30g/L tartaric acid. The present study validates the beneficial role of 30g/L tartaric acid in anodizing electrolyte for the growth of anodic film on titanium alloy.

Keywords: tartaric acid; pulse anodic oxidation; Ti-6.5Al-1Mo-1V-2Zr

1. INTRODUCTION

Ti-6.5Al-1Mo-1V-2Zr is a titanium alloy that is widely used in the aerospace and transport industries because of high strength and excellent creep resistance [1]. Due to severe service environments, anodic films are required to improve the corrosion resistance[2]. Depending on electrolytes, different anodic films are obtained. Sulfuric acids with different degrees of dilution, for instance, are the most commonly used electrolytes in titanium anodizing. Much research has been focused on the relation between sulfuric acid electrolyte and surface morphologies and corrosion resistance of the film [3, 4].

Compared with titanium anodizing, aluminum anodizing in acid electrolytes has been largely studied [5]. For aluminum anodizing, in order to replace hazardous chromic acids, organic acids are added to sulfuric acid to improve the anticorrosion performance of aluminum alloy. Corrosion resistance of the specimens anodized in sulfuric acid/boric acid is satisfactory and fatigue resistance

after anodizing is almost same as that obtained with traditional chromic acid anodizing [6]. Other electrolytes are also investigated using mixed acids, such as tartaric acid/ sulfuric acid [7]. Specially, tartaric acid is added to sulfuric acid to improve the corrosion resistance of aluminum alloy by influencing the field-assisted dissolution process, limiting the dissolution of the anodic film in the pore walls[8]. However, few data of anodic oxidation of the titanium alloy in tartaric acid / sulfuric acid (TSA) are available and experimental procedures are still needed to be developed.

Parameters, such as electrical potential [9], electrolyte solution [10], frequency [11], and composition of substrate [12] affect the characteristics of anodic film on titanium alloy. Among these parameters, the concentration of electrolyte solution was studied carefully to make sure that the oxide growth rate is higher than the dissolution one. Excessive amount or deficiency leads to the decrease of the anodic layer properties. Proper growth rate for anodic film is very important to avoid deficiency of the anodic film. Therefore, it is necessary to optimize the concentration of electrolyte in order to obtain anodic film with good corrosion resistance [13].

In the present work, the effect of tartaric acid on microstructure and corrosion resistance of sulfuric acid anodic film on Ti-6.5Al-1Mo-1V-2Zr titanium alloy has been investigated by Scanning electron microscopy (SEM), Raman spectra, and electrochemical technique. Specially, different amounts of tartaric acid were added to sulfuric acid and the morphology of resultant anodic films was examined.

2. EXPERIMENTAL

2.1 Material and procedure.

Pulse anodic oxidation was carried out on forged titanium alloy Ti-6.5Al-1Mo-1V-2Zr, which was cut into dimensions of 10mm×10mm×2mm. The nominal chemical components of titanium alloy Ti-6.5Al-1Mo-1V-2Zr are shown in Table 1. Prior to pulse anodizing, samples were abraded with silicon carbide paper successively grades from 200 to 2000 grit and then ultrasonically cleaned in acetone solution.

Table 1. Nominal chemical components of Ti-6.5Al-1Mo-1V-2Zr titanium alloy (wt%)

Al	**Mo**	**V**	**Zr**	**Fe**	**C**	**N**	**O**	**Ti**
5.5~7.1	0.5~2.0	0.8~2.5	1.5~2.5	＜0.25	＜0.08	＜0.05	＜0.15	Balance

Anodic films of the samples were obtained by using pulse galvanostatic power source (WMY-V) in a cell with a thermostat water bath and a magnetic stirring apparatus. Pt electrode (5 cm × 5 cm) was used as the cathode. 10, 30, 50, 70, 90g/L tartaric acid were added to 184g/L sulfuric acid, and the electrolytes are named as T_1SA, T_2SA, T_3SA, T_4SA and T_5SA, respectively. The parameters of anodic

oxidation were given in the Table 2. After anodizing, three anodized substrates were immersed into sulfuric acid and sulfuric acid with different tartaric acid additions.

Table 2. Parameters of anodic oxidation

Parameters	Value
Current density/(A•dm^{-2})	5
Sulfuric acid concentration/(g•L^{-1})	184
Temperature/(K)	293
Duty ratio/(%)	20
Frequency/(freq/min)	60
Tartaric acid/(g•L^{-1})	0,10,30,50,70,90
Anodizing time/(min)	50

2.2 Surface analysis.

Scanning electron microscopy (SEM, Hitachi S-4800) was used to examine cross-section morphology and thickness of the oxide films. The crystalline structure of oxide films was measured by Raman spectroscopy (Raman, Nanophoton Raman-11, He–Ne laser without filter, 532 nm).

2.3 Electrochemical measurement.

The electrochemical experiments were examined in a traditional three-electrode system using a potentiostat/galvanostat (Parstat 2273, Princeton Applied Research, USA) in 3.5%wt NaCl solution. The sample (1cm^2) was the working electrode of the system, with a saturated calomel electrode reference electrode and a pure platinum electrode counter-electrode. Electrochemical impedance spectra (EIS) were carried out after monitoring the open circuit potential (OCP) for approximately 1 h until steady values were achieved at room temperature; Electrochemical impedance spectra (EIS) were recorded in the frequency range between 100 kHz and 10 mHz with AC signal of 10 mV amplitude.

3. RESULTS AND DISCUSSION

3.1 Effect of tartaric acid concentration on the surface morphology and cross-section of anodized titanium alloy

Fig. 1 displays SEM surface morphology of samples anodized in sulfuric acid without tartaric acid and with different tartaric acid additions. Cavities revealed in Fig .1 indicate that sulfuric acid was aggressive towards the growing oxide. The cavities were the characteristic morphology of films formed in the sulfuric acid. Obviously, in the tartaric acid/sulfuric acid, the anodizing process was not a uniform one because of different anodizing characteristics of α-phase and β-phase. This may be due

to that β-phase was rich in vanadium and that vanadium oxides had high solubility in sulfuric acid. Thus, porous layer tended to grow at the zone of β-phase during the initial stage of anodic oxidation. The results are in good accordance with other study concerning the anodic oxidation of bi-phase titanium alloy [14]. In addition, when tartaric acid concentration was 30g/L, the surface of anodic film was smoothest.

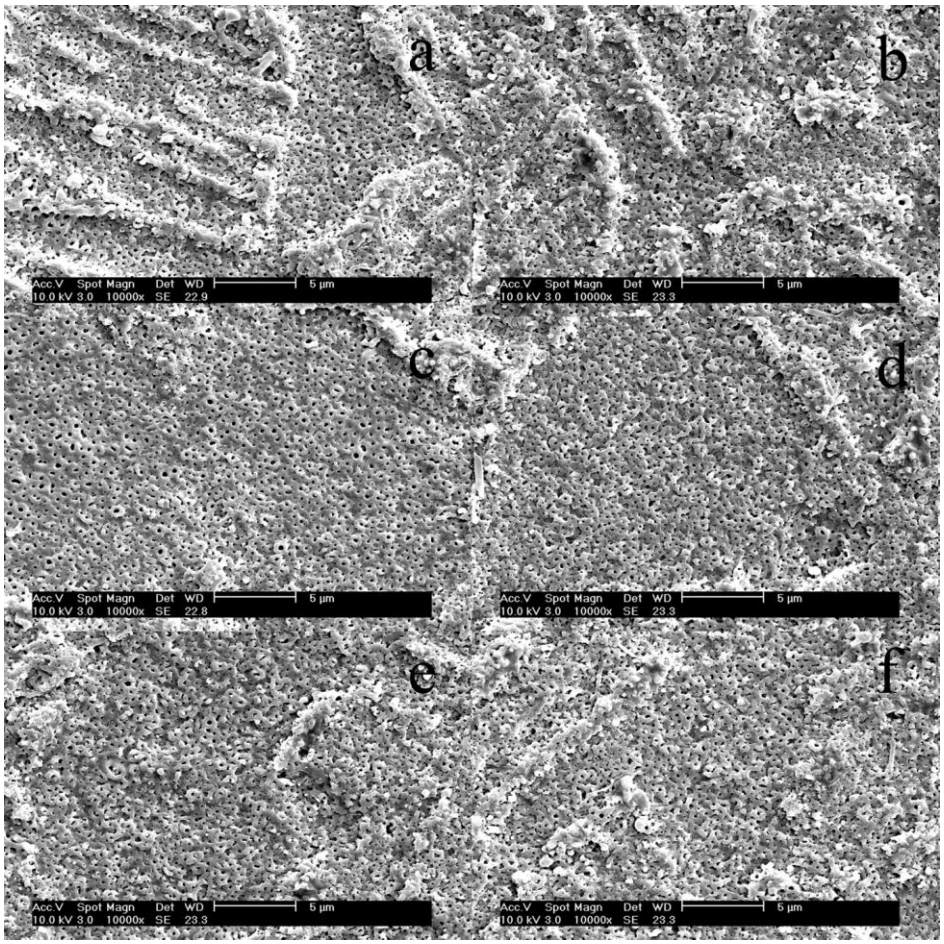

Figure 1. SEM images of titanium alloy anodised in sulfuric acid without tartaric acid (a) and with 10g/L tartaric acid (b), 30g/L tartaric acid (c), 50g/L tartaric acid (d), 70g/L tartaric acid (e) and 90g/L tartaric acid (f).

The cross-section morphology of anodic film of the titanium alloy is shown in Fig. 2. Usually, under the galvanostatic mode, the thickness of the film is determined by the current density [15]. Though the porous layer and barrier layer were not clearly distinguished in the SEM images, but the oxide film thickness, associated with similar current density, varied with the increasing tartaric acid concentrations. Thicknesses of the anodic film were marked in Fig 1. When the tartaric acid concentration was increased to 30g/L, the thicknesses was enlarged to 2.0μm. However, the thicknesses of anodic film were reduced with further increasing tartaric acid concentration.

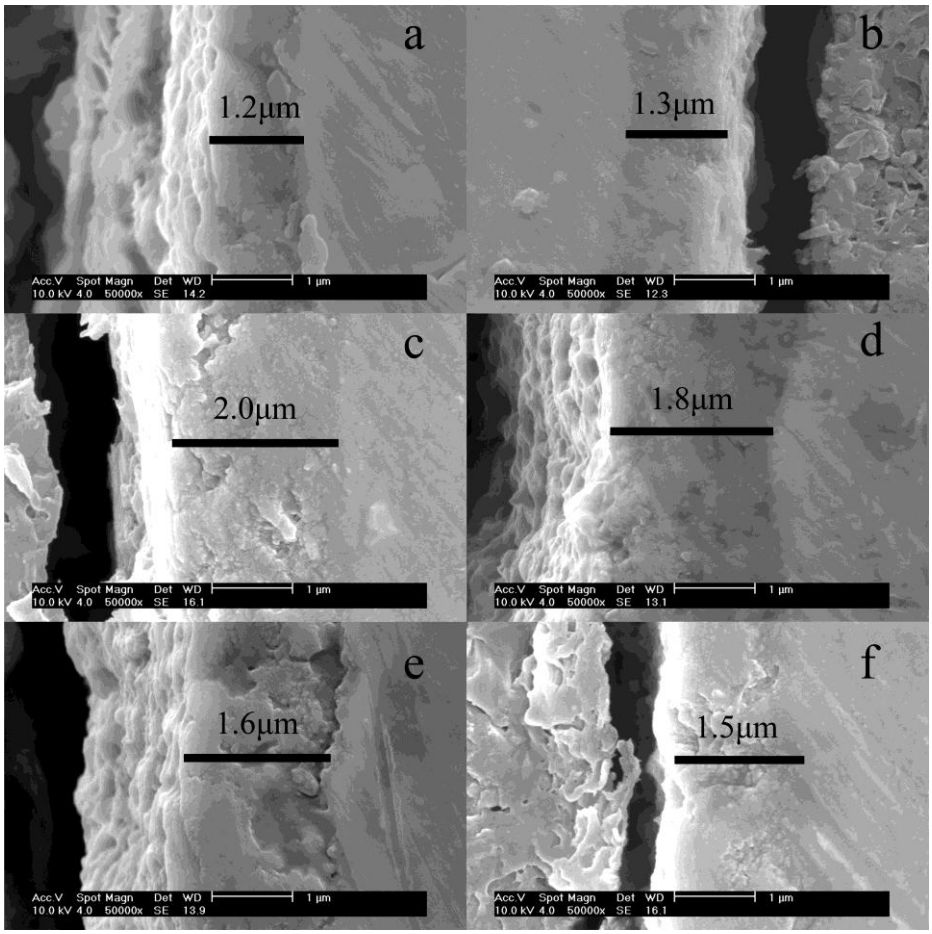

Figure 2. SEM images of titanium alloy anodised in sulfuric acid without tartaric acid (a) and with 10g/L tartaric acid (b), 30g/L tartaric acid (c), 50g/L tartaric acid (d), 70g/L tartaric acid (e) and 90g/L tartaric acid (f).

3.2 Effect of tartaric acid concentration on the crystallinity of titanium alloy anodic film

Fig. 3 presents the Raman spectra of titanium alloy anodic films obtained in sulfuric acid without tartaric acid and with different tartaric acid additions. The spectra were similar and exhibited three peaks at 235.5 (E_g), 445.8 cm^{-1}(E_g) and 609.5 cm^{-1}(A_{1g}), which were assigned to the Raman-active modes of rutile. In addition, the spectra also presented two dominate peaks at 519 cm^{-1}(A_{1g}, B_{1g}) and 144 cm^{-1}(E_g), which belonged to that of anatase [16, 17]. The appearance of strongest peak intensity at 144 cm^{-1} is due to that the dominant peak of anatase and rutile located around the same Raman shift, which is around 144 cm^{-1}. The results concurred with result obtained by other literature [18]. Thus, oxide film of all samples contained both rutile and anatase.

The areas of the strongest Raman peak at 144cm^{-1} are showed in Fig. 4. Generally, the crystallization degree of anodic films on titanium alloy can be roughly calculated using the following equation:

$$\theta = \frac{\mu A}{d} \qquad (1)$$

where μ represents the peak area of Raman spectra at 144 cm^{-1}, θ is the crystallinity of titanium oxide films, d represents the film thickness, and A is a constant which is set as 1 nm/a.u. here. The values of θ calculated of both SA and TSA are showed in Fig. 4. It is obvious that the crystallinity of titanium alloy anodic film firstly decreased and then increased with the increasing tartaric acid concentration.

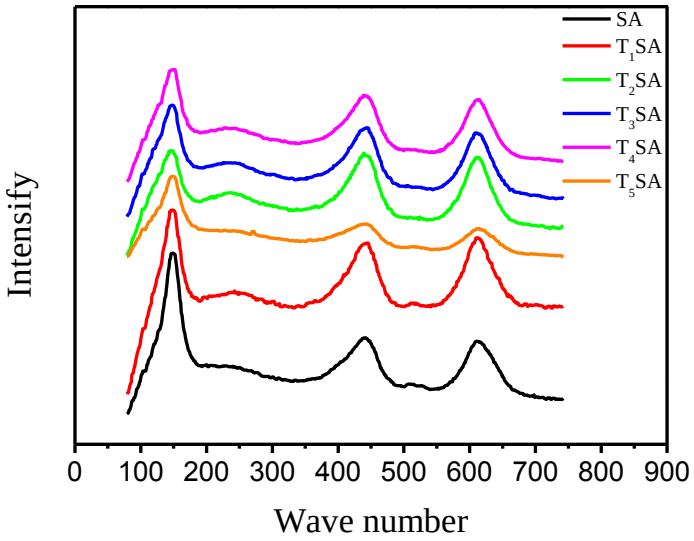

Figure 3. Raman spectra of anodic films formed in sulfuric acid without tartaric acid (SA) and sulfuric acid with 10g/L (T_1SA), 30g/L (T_2SA), 50g/L (T_3SA), 70g/L (T_4SA) and 90g/L (T_5SA) tartaric acid.

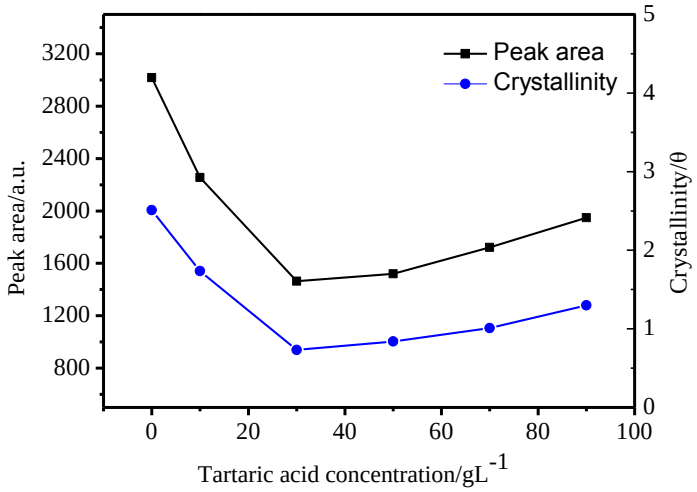

Figure 4. Crystallinity of anodic film formed in sulfuric acid and sulfuric acid with different tartaric acid additions.

During growth, oxygen ions that migrate inward can lose their electrons and be converted to molecular oxygen during migration process, producing gas bubbles that are confined in the film. This is due to following equation:

$$O^{2-} - 2e^{-} = O_2 \quad (2)$$

This phnomenon has been observed by transmission electron microscope (TEM) during anodizing of titanium[12]. The growth of an oxygen bubble often occurs in crystalline region, which was corroborated by Mazzarolo[3]. This is due to that, under galvanostatic conditions, the amorphous to crystalline transition takes place at some stages of film growth. The crystallization resulted in high electronic conductivity, which enabled oxygen evolution on crystalline regions to take place[19]. As the crystalline phase nucleated, oxygen evolution of the anodic film was triggered. Thus, the presence of crystalline phase in anodic film could promote the oxygen evolution within the anodic film. However, when tartaric acid addition was 30g/L, crystallinity of anodic film was lowest. Therefore, the intensity of oxygen evolution of anodic film formed in sulfuric acid with 30g/L tartaric acid was lowest.

3.3 Effect of tartaric acid concentration on the dissolution rate of anodizing film.

Different dissolution rate among samples in sulfuric acid and sulfuric acid with different tartaric acid additions may engender the variation of thicknesses of specimens. In order to investigate the dissolution rate, the samples were anodized in sulfuric acid without the presence of tartaric acid and then immersed in sulfuric acid and sulfuric acid with tartaric acid concentrations for 24 hours.

Impedance measurements were performed on specimens after 24 hours immersion and results are shown in Fig. 5. Though two time constants still existed in Fig. 5(b), the effect of immersion in the sulfuric acid and sulfuric acid with tartaric acid was evidenced by the decrease of the impedance modulus (|Z|), particularly in medium and high regions of the diagram. This was indicative that significant degradation of the porous layers was taking place. The relative high impedance modulus in low frequency ranges for sample immersed in sulfuric acid with 30g/L tartaric acid revealed that 30g/L tartaric acid addition produced the slowest dissolution rate towards the oxide films among all solutions.

Qualitative comparison of the impedance data provides further comprehension to the responses of anodized specimens. Simplified equivalent circuit was used to simulate the conditions expected on the titanium alloys surface and to analyze impedance data obtained from Fig. 5. In this paper, an equivalent circuit (EC) with two RC components [20, 21] was used and shown in Fig. 6. The circuit consists of follow elements: resistance R_{el} of the test electrolyte, resistance R_p and the constant phase elements (CPE) Q_p of porous layer, resistance R_b and the constant phase elements (CPE) Q_b of the barrier layer. Specially, CPE was selected due to the case of capacitance affected by the distribution of the relaxation frequency [22]. The impedance results were extracted with the ZSimpWin software.

Capacitance (C) can be obtained by using:

$$C=(R^{1-n} Q)^{1/n} \quad (3)$$

where R represents parallel resistance, Q is constant phase elements, and the value of the exponent n, ranging $-1 \leq n \leq 1$, indicates the deviation from ideal capacitive behaviour. The thickness of anodic film (d) can be calculated by using :

$$d=\frac{A \varepsilon \varepsilon_0}{C} \quad (4)$$

where ε is the dielectric constant of the anodic film, ε_0 the vacuum permittivity, A the geometric area, and d is the thickness.

The dissolution rate of anodic film can be estimated by using follow equation:

$$v=\frac{\Delta d}{\Delta t}=\frac{\Delta\left(\varepsilon\,\varepsilon_0 A/\,C\right)}{\Delta t}=\varepsilon\,\varepsilon_0\,A\frac{\Delta\left(1/\,C\right)}{\Delta t} \quad (5)$$

where d is the thickness and t is immersion time. Here, we assume :

$$K=\frac{\Delta\left(1/\,C\right)}{\Delta t}=\frac{v}{\varepsilon\,\varepsilon_0 A} \quad (6)$$

Therefore, we can use the value of K to estimate the dissolution rate of anodic film. From the fitted data showed in Table. 3, the value of K of all samples can be obtained. When tartaric acid concentration was 30g/L, the dissolution rate of solution was slowest.

Table 3. Results of simplified equivalent circuit of samples immersed in sulfuric acid and sulfuric acid with different tartaric acid additions.

Tartaric acid addition/gL^{-1}	R_p /Ω cm^2	Q_p / $10^{-6}s^n$ Ω cm^{-2}	n
Without immersion	5079	12.2	0.842
0	4584	617.2	0.862
10	72760	270.7	0.817
30	13260	40.48	0.761
50	19130	50.93	0.732
70	47950	192.8	0.783
90	24530	289.7	0.781

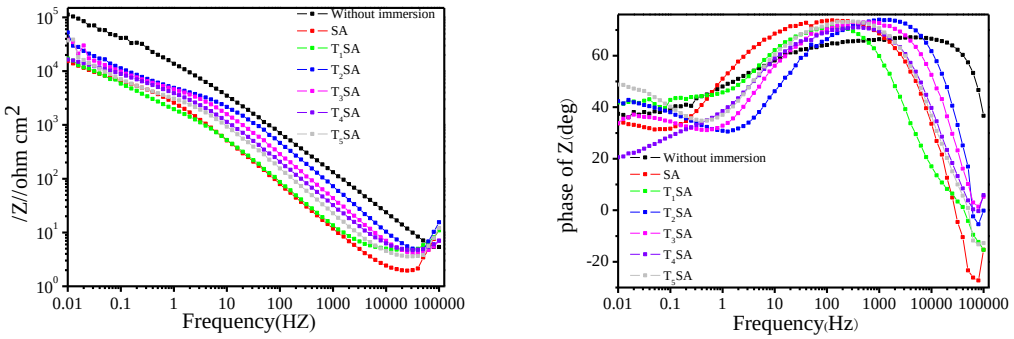

Figure 5. Impedance response (a) and phase shift (b) of anodic film immersed in sulfuric acid (SA) and sulfruric acid with 10g/L tartaric acid (T_1SA), 30g/L tartaric acid (T_2SA), 50g/L tartaric acid (T_3SA), 70g/L tartaric acid (T_4SA), 90g/L tartaric acid (T_5SA).

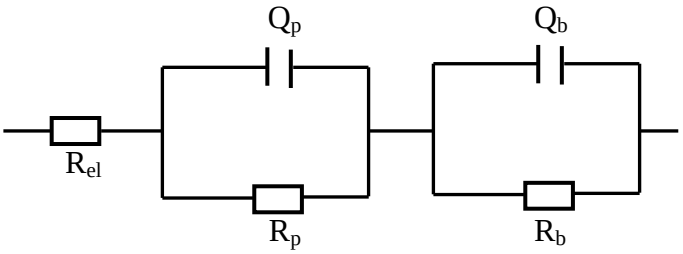

Figure 6. simplified equivalent circuit used to model electrochemical behavior.

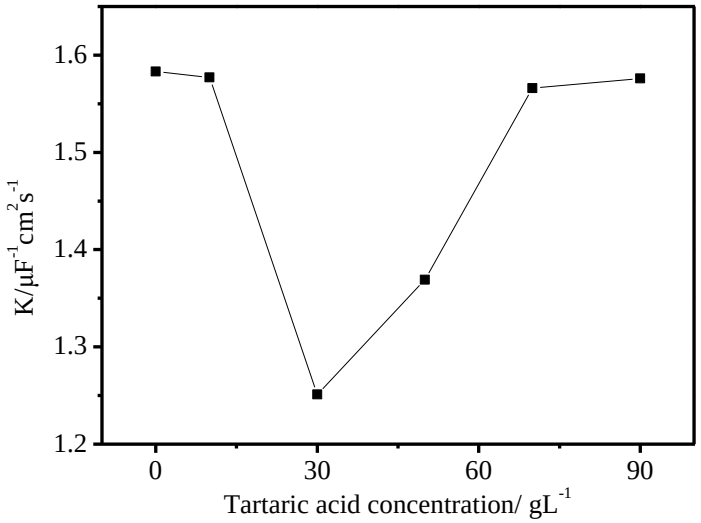

Figure 7. Dissolution rate of anodic film immersed in sulfuric acid and sulfuric acid with different tartaric acid additions.

For titanium anodic oxidation in potentiostatic mode, the current can be consumed in the film formation, the film dissolution and the oxygen evolution process[23]. Here, we could compare film formation current density of all samples using:

$$I_f=I_a-I_d-I_O \quad (3)$$

where I_f represents the formation current density, I_a is applied current density, I_d is the film dissolution current density, and I_O represents the applied current density that is used for the oxygen evolution. Under the galvanostatic mode, the value of I_a is fixed. Here, when tartaric acid concentration was 30g/L, the oxygen evoltuion in the pores of anodized samples and dissoltuion rate of anodic film were smallest. Therefore, the growth rate of anodic film formed in sulfuric acid with 30g/L tartaric acid was fastest. In fact, tartaric acid has a strong tendency to combine with titanium ions to produce titanium tartarte and titanium tartarte is highly soluble in acidic solution. This lead to the further dissolution of anodic film. At this point, the tartaric acid serves as solvent. During anodizing, tartrate species are assumed to be adsorbed on the pore wall material. The presence of tartrate anions in pores prevents the pH from decreasing to very low values when relatively high concentrations of H_2SO_4 are present. From the corrosion viewpoint, this effect is beneficial because local acidification

corresponding to active anodic sites may be reduced by the presence of tartrate species. The presence of tartaric species in pores plays a protective role. Therefore, the tartaric acid serves as both solvent and protection agents. When the concentration of tartaric aid is 30g/L, the protection effects exceed dissolution effects. However, when the concentration is 90g/L, protection effects were weakened by the dissolution effects.

4. CONCLUSIONS

(1) For Ti-6.5Al-1Mo-1V-2Zr titanium alloy, porous tended to grow at the zone of β-phase than α-phase during anodic oxidation. When tartaric acid concentration was 30g/L, the surface of anodic film was smoothest.

(2) When tartaric acid concentration was 30g/L, the anodic film had lowest crystallinity and slowest dissolution rate. Therefore, the presence of 30g/L tartaric acid in sulfuric acid increased the growth rate of the oxide film on titanium alloy.

ACKNOWLEDGEMENT
This work was supported by the National Natural Science Foundation of China (No. 51271012).

Reference

1. R. Boyer, *Mater. Sci. Eng.*, 213 (1996) 103-114.
2. B. Arifvianto, Suyitno and M. Mahardika, *Int J Miner Metall Mater*, 20 (2013) 788-795.
3. A. Mazzarolo, M. Curioni, A. Vicenzo, P. Skeldon and G. Thompson, *Electrochim. Acta*, 75 (2012), 288-295.
4. J. Zhan, Q.j. Luo, Y. Huang and X.d. Li, *Int J Miner Metall Mater*, 21 (2014), 925-933.
5. N. DU, S.x. WANG, Q. ZHAO and Z.s. SHAO, *Trans. Nonferrous Met. Soc. China*, 22 (2012) 1655-1660.
6. L. Domingues, J. Fernandes, M. Da Cunha Belo, M. Ferreira and L. Guerra-Rosa, *Corros. Sci.*, 45 (2003) 149-160.
7. M. García-Rubio, P. Ocón, A. Climent-Font, R. Smith, M. Curioni, G. Thompson, P. Skeldon, A. Lavía and I. García, *Corros. Sci.*, 51 (2009) 2034-2042.
8. G. Boisier, N. Pébère, C. Druez, M. Villatte and S. Suel, *J. Electrochem. Soc.*, 155 (2008), 521-529.
9. S.n. Wang, Y. Li and T.t. Zhao, *Int J Miner Metall Mater*, 19 (2012), 1134-1141.
10. M. Diamanti and M. Pedeferri, *Corros. Sci.*, 49 (2007), 939-948.
11. S. Li, X. Yu, J. Liu, M. Yu, G. Wu, L. Wu and K. Yang, *Int. J. Electrochem. Sci.*, 8 (2013), 5438-5447.
12. H. Habazaki, M. Uozumi, H. Konno, S. Nagata and K. Shimizu, *Surface and Coatings Technology*, 169 (2003) 151-154.
13. W. Bensalah, K. Elleuch, M. Feki, M. Wery and H. Ayedi, *Surf. Coat. Technol.*, 201 (2007), 7855-7864.
14. E. Matykina, J. M. Hernandez-López, A. Conde, C. Domingo, J. J. de Damborenea and M. A. Arenas, *Electrochim. Acta*, 56 (2011), 2221-2229.
15. A. Cigada, M. Cabrini and P. Pedeferri, *J. Mater. Sci. - Mater. Med.*, 3 (1992), 408-412.

16. J. Castro, M. López-Ramírez, J. Arenas and J. Otero, *Vib. Spectrosc*, 39 (2005), 240-243.
17. J. Surmacki, P. Wroński, M. Szadkowska-Nicze and H. Abramczyk, *Chem. Phys. Lett.*, 566 (2013) 54-59.
18. U. Balachandran and N. Eror, *J. Solid State Chem.*, 42 (1982) 276-282.
19. M. T. Tanvir, K. Fushimi, K. Shimizu, S. Nagata, P. Skeldon, G. Thompson and H. Habazaki, *Electrochim. Acta*, 52 (2007) 6834-6840.
20. V. Moutarlier, M. Gigandet, B. Normand and J. Pagetti, *Corros. Sci.*, 47 (2005) 937-951.
21. J. Fojt, *Appl. Surf. Sci.*, 262 (2012) 163-167.
22. T. Pauporte and J. Finne, *J. Appl. Electrochem.*, 262 (2006) 33-41.
23. J. Xing, Z. Xia, J. Hu, Y. Zhang and L. Zhong, *Corros. Sci.*, 36 (2013), 212-219.